Published in final edited form as:

Circulation. 2017 July 04; 136(1): 83–97. doi:10.1161/CIRCULATIONAHA.116.025889.

Melanocortin 1 Receptor Signaling Regulates Cholesterol Transport in Macrophages

Petteri Rinne, PhD[1,2], **Martina Rami, MSc**[1], **Salla Nuutinen, MSc**[2], **Donato Santovito, MD, PhD**[1], **Emiel P.C. van der Vorst, PhD**[1], **Raquel Guillamat-Prats, PhD**[1], **Leo-Pekka Lyytikäinen, MD, PhD**[3], **Emma Raitoharju, PhD**[3], **Niku Oksala, MD, PhD, DSc**[3,4], **Larisa Ring, PhD**[1], **Minying Cai, PhD**[5], **Victor J. Hruby, PhD**[5], **Terho Lehtimäki, MD, PhD**[3], **Christian Weber, MD**[1,6], and **Sabine Steffens, PhD**[1,6]

[1]The Institute for Cardiovascular Prevention (IPEK), Ludwig-Maximilians-University (LMU) Munich, Munich, Germany [2]The Department of Pharmacology, Drug Development and Therapeutics, University of Turku and Turku University Hospital, Turku, Finland [3]Department of Clinical Chemistry, Fimlab Laboratories and Faculty of Medicine and Life Sciences, University of Tampere, Tampere, Finland [4]Department of Surgery, Tampere University Hospital, Tampere, Finland [5]The Department of Chemistry and Biochemistry, University of Arizona, Tucson, Arizona, USA [6]The German Centre for Cardiovascular Research (DZHK), Partner Site Munich Heart Alliance, Munich, Germany

Abstract

Background—The melanocortin 1 receptor (MC1-R) is expressed by monocytes and macrophages, where it exerts anti-inflammatory actions upon stimulation with its natural ligand α-melanocyte-stimulating hormone (α-MSH). The present study was designed to investigate the specific role of MC1-R in the context of atherosclerosis and possible regulatory pathways of MC1-R beyond anti-inflammation.

Methods—Human and mouse atherosclerotic samples and primary mouse macrophages were used to study the regulatory functions of MC1-R. The impact of pharmacological MC1-R activation on atherosclerosis was assessed in apolipoprotein E deficient ($ApoE^{-/-}$) mice.

Results—Characterization of human and mouse atherosclerotic plaques revealed that MC1-R expression localizes in lesional macrophages and is significantly associated with the ATP-binding cassette transporters ABCA1 and ABCG1, which are responsible for initiating reverse cholesterol transport. Using bone marrow-derived macrophages, we observed that α-MSH and selective MC1-R agonists similarly promoted cholesterol efflux, which is a counter-regulatory mechanism against foam cell formation. Mechanistically, MC1-R activation upregulated the levels of ABCA1 and ABCG1. These effects were accompanied by a reduction in cell surface CD36 expression and in cholesterol uptake, further protecting macrophages from excessive lipid accumulation. Conversely, macrophages deficient in functional MC1-R displayed a phenotype with impaired efflux and

Correspondence: Petteri Rinne, Department of Pharmacology, Drug Development and Therapeutics, University of Turku, Kiinamyllynkatu 10, 20520 Turku, Finland, Phone: +358-2-333-7605, Fax: +358-2-333-7216, pperin@utu.fi.

Disclosures: None

enhanced uptake of cholesterol. Pharmacological targeting of MC1-R in atherosclerotic ApoE$^{-/-}$ mice reduced plasma cholesterol levels and aortic CD36 expression as well as increased plaque ABCG1 expression and signs of plaque stability.

Conclusions—Our findings identify a novel role for MC1-R in macrophage cholesterol transport. Activation of MC1-R confers protection against macrophage foam cell formation through a dual mechanism: it prevents cholesterol uptake while concomitantly promoting ABCA1- and ABCG1-mediated reverse cholesterol transport.

Keywords

atherosclerosis; macrophage; melanocortin 1 receptor; cholesterol homeostasis; inflammation

INTRODUCTION

The melanocortin system, consisting of melanocyte-stimulating hormones (α, β and γ-MSH) and their cognate receptors, regulates a variety of physiological functions, ranging from skin pigmentation to centrally mediated energy balance control.[1,2] At the cellular level, the biological actions are mediated by a family of five G-protein coupled melanocortin receptors, named from MC1-R to MC5-R, which all have distinct tissue distribution and functional properties. MC1-R was the first receptor member to be cloned and is known to be an integral regulator of skin pigmentation.[3,4] Over the past years it has become evident that MC1-R signaling exerts not only melanogenesis in the skin but also immunomodulatory effects through its wide expression in the cells of the immune system like monocytes and macrophages.[1,5,6] However, since macrophages also express MC3-R which is proposed to be the dominant receptor over MC1-R for conveying melanocortin-induced anti-inflammation,[7–9] the question arises whether MC1-R is dispensable in this regard or whether it may exhibit additional yet unknown functions in macrophages. To address these questions, we investigated the role of MC1-R in the context of atherosclerosis with particular focus on cholesterol metabolism, which is a crucial function of macrophages.

Atherosclerosis is a chronic inflammatory disease of large and medium-sized arteries that involves both the innate and adaptive immune systems.[10,11] In particular, monocytes and their descendant macrophages are the dominant effector cells responsible for the disease initiation and progression.[12–14] Hypercholesterolemia and increased plasma levels of the principal atherogenic lipoprotein, low-density lipoprotein (LDL), promote cholesterol trapping and accumulation in the arterial intima, which eventually attracts monocytes to the scene. Under oxidative conditions, LDL becomes modified, enabling its recognition and uptake by macrophages *via* scavenger receptors. When macrophages engulf oxidized LDL (oxLDL), it directly triggers pro-inflammatory signaling pathways and secondly, it drives the transformation of these cells into foam cells, which in turn, amplifies the inflammatory process and aggravates atherosclerosis.[15] This detrimental cascade is counter-regulated by reverse cholesterol transport, which facilitates the clearance of excess cholesterol from macrophages and its subsequent transport to the liver for excretion. The first steps of reverse cholesterol transport are mediated by the ATP-binding cassette transporters ABCA1 and ABCG1, which promote cholesterol efflux onto high-density lipoprotein (HDL) particles and its main protein constituent apolipoprotein A1 (ApoA1). Consequently, fine-tuning the

balance between cholesterol uptake and efflux protects against maladaptive immune responses, foam cell formation and ultimately against atherosclerosis.

Given the previously identified expression of MC1-R in macrophages, the major cell type within atherosclerotic plaques, we first aimed to characterize MC1-R expression in human and mouse atherosclerosis. We confirmed colocalization of MC1-R expression with macrophages in atherosclerotic lesions and found strong positive correlation with the expression of reverse cholesterol transporters rather than with inflammatory markers. Thus, we hypothesized that MC1-R signaling is involved in the regulation of cholesterol transport in macrophages.

METHODS

Detailed methods are available in the Data Supplement.

Mice

Adult C57Bl/6J (Janvier Labs) and MC1-R deficient (Jackson Laboratory, strain# 000060) mice were used to obtain bone marrow-derived macrophages (BMDM). For atherosclerosis studies, apolipoprotein E-deficient ($ApoE^{-/-}$) were randomly assigned to receive daily i.p. injections of either PBS (vehicle) or the selective MC1-R agonist MSG606 (1mg/kg),[16] and were fed a cholesterol-rich high-fat diet for 4 weeks. All animal experiments were approved by the local ethics committees and conducted in accordance with the institutional and national guidelines for the care and use of laboratory animals.

Human Endarterectomy Samples

Tampere Vascular Study (TVS) endarterectomy samples were obtained from carotid arteries, abdominal aortas and femoral arteries as previously described.[17,18] The left internal thoracic artery (LITA) samples, obtained during coronary artery bypass surgery, served as controls. Gene expression was analyzed from carotid (n=29), abdominal aortic (n=15), and femoral (n=24) plaques, and atherosclerosis-free LITAs (n=28). The expression levels were analyzed with Illumina HumanHT-12 v3 Expression BeadChip (Illumina).[18,19] The study was approved by the Ethics Committee of Tampere Hospital District and conducted according to the declaration of Helsinki, and the study subjects gave informed consent.

Bone Marrow-Derived Macrophages

Bone marrow cells were cultured in RPMI-1640 medium supplemented with 10% FCS, penicillin (100U/mL), streptomycin (100μg/mL) (all Gibco Life Technologies) and 10% filtered L-929 cell-conditioned medium as a source of M-CSF. Experiments were done on differentiated bone marrow-derived macrophages (BMDMs) 7 to 10 days after plating.

Flow Cytometry Analysis of BMDMs

To assess the uptake of oxLDL, BMDMs were treated with Dil-conjugated oxLDL (5–20μg/mL, Alfa Aesar) for 4h and then analyzed with FACS Canto II (BD Biosciences). To quantify the expression of CD36 on the cell surface, BMDMs were stained with antibodies against CD36 PE-Cy7 (clone HM36) and CD11b APC (clone M1/70). Proliferation and cell

cycle status was assessed after staining with Ki67 FITC (clone SolA15) and the nuclear DNA dye 7-aminoactinomycin D (7-AAD).

Cholesterol Efflux Assay

BMDMs were incubated with complete medium containing [^{3}H]-cholesterol (1μCi/well, PerkinElmer) and oxLDL (20μg/mL, Alfa Aesar) for 24h and thereafter equilibrated for 18h in RPMI medium containing 0.2% BSA. When stated, the cells were treated with α-MSH or the selective MC1-R agonists during the equilibration phase. The equilibrated BMDMs were then incubated for 6h with serum-free RPMI medium containing 0.2% BSA and ApoA1 (15μg/mL, Sigma) or HDL (50μg/mL, Millipore) to facilitate cholesterol efflux.

Western Blotting

BMDMs were lysed using RIPA buffer, size-fractioned by SDS-polyacrylamide gel electrophoresis and then transferred to nitrocellulose membranes. After blocking step, membranes were probed with primary antibodies followed by detection with HRP-conjugated secondary antibodies and enhanced chemiluminesence. Target protein expression was normalized to glyceraldehyde-3-phosphate dehydrogenase (GAPDH) or β-actin to correct for loading.

Quantitative Real-Time PCR

Total RNA was extracted (peqGold Trifast and Total RNA kit, Peqlab) and reverse transcribed (PrimeScript RT kit, Clontech). Real-time PCR was performed with the 7900HT Sequence Detection System (Applied Biosystems) using predesigned primer and probe mix (Life Technologies) or primer sequences given in Supplemental Table I. Target protein expression was normalized to hypoxanthine phosphoribosyltransferase (HPRT) and the fold induction was calculated using the comparative ΔCt method and are presented as relative transcript levels ($2^{-\Delta\Delta Ct}$).

Histology and Immunohistochemistry

Aortic roots were cut in 5 μm-thick serial cryosections and stained with Oil-Red-O to quantify lesion size. For immunohistochemisty, sections were incubated with primary antibodies (against MC1-R, ABCG1, Mac-2 or CD68) and subsequently with a horseradish peroxidase-conjugated secondary antibody and diaminobenzidine (ABC kit, Vector Labs) or with fluorochrome-conjugated secondary antibodies.

Flow Cytometry

Aorta, spleen, bone marrow and blood samples from ApoE$^{-/-}$ mice were used for quantification of leukocyte subsets by flow cytometry. After preparation of single cell suspensions, cells were stained with fluorochrome-conjugated antibodies against CD45.2 (clone 104), CD11b (clone M1/70), CD115 (clone AFS98), F4/80 (clone BM8), Ly6C (clone AL-21) and Ly6G (clone 1A8), and were measured by FACS Canto II flow cytometer.

Statistical Analysis

Statistical analyses were performed with GraphPad Prism 5 (GraphPad Software Inc.) or R version 3.1.1 (http://www.r-project.org/). For comparisons of MC1-R expression in human samples, log-transformed data and the nonparametric Mann Whitney U test were used. Pearson or nonparametric Spearman correlation coefficients were calculated for gene associations based on D'Agostino-Pearson ominibus normality test results. For mouse data, Student's t test, Mann Whitney U test or one-way ANOVA was used to determine statistical significance. For two independent factors, two-way ANOVA was used followed by Bonferroni *post hoc* tests. Possible outliers in the data sets were detected using the robust regression and outlier removal (ROUT) method at Q-level of 5%. All data are presented as mean ± standard error of the mean (SEM). A two-tailed P value of <0.05 was considered statistically significant.

RESULTS

Human and Mouse Atherosclerotic Plaques Express MC1-R in Macrophage-Rich Areas

We first screened the expression of melanocortin receptor subtypes in human endarterectomy samples and compared the transcript levels to atherosclerosis-free control arteries (left internal thoracic artery; LITA). Strikingly, MC1-R was the only subtype that showed consistent and highly significant expression changes in different types of endarterectomy samples compared to controls (Supplemental Table II). MC1-R was markedly upregulated (fold change 1.7, P=1.3e-11) in atherosclerotic plaques (Figure 1A), but the expression did not differ between stable and unstable plaque types (Figure 1B). The expression of MC1-R in endarterectomy samples was further confirmed with immunohistochemical stainings (Figure 1C and 1D), which also revealed that MC1-R staining merged with CD68-positive area (Figure 1D), indicative of colocalization in monocytes/macrophages. Supporting this finding, gene association analyses using all plaque samples indicated that MC1-R positively correlated with macrophage markers and negatively with smooth muscle cell signature (Supplemental Figure 1). When analyzing gene associations separately in samples from different origins, we observed that MC1-R expression particularly correlated with classical pro-inflammatory markers (IL1β, TNFα and CCL2) in carotid plaque samples (Figure 1E), while no clear pattern of correlations with M1- or M2-type macrophage markers appeared in femoral (Figure 1F) or abdominal (data not shown) plaque samples. Interestingly, further screening of carotid samples uncovered that MC1-R expression significantly associated with the reverse cholesterol transporters ABCA1 and ABCG1 as well as with the scavenger receptor class B member 1 (SR-BI, also known as SCARB1), which facilitates bidirectional cholesterol fluxes in macrophages (Figure 1G–1I). No significant correlations with other scavenger receptors like CD36 and SR-A (also known as MSR1) were noted (Figure 1J and 1K).

We further sought to investigate the expression pattern of MC1-R in atherosclerotic lesions and in other tissues of ApoE$^{-/-}$ mice at different stages of the disease. Shifting from normal chow diet to atherogenic high-fat diet (HFD) caused a robust upregulation of MC1-R expression in the aorta after 4 weeks of HFD, which then declined towards a more advanced stage of atherosclerosis (Figure 2A). This expression pattern might not be simply explained

by the accumulation of macrophages within the aortic wall, because macrophages also represent the predominant cell type at advanced plaque stage. Thus, we hypothesized that a shift in macrophage phenotype might lead to a change in MC1-R expression. *In vitro* experiments with BMDMs indeed revealed lower protein levels of MC1-R when macrophages were polarized with IL-4 or dexamethasone into an M2 phenotype (Supplemental Figure 2A). However, MC1-R protein levels were unaffected by exposure to increasing doses of either native LDL or oxLDL (Supplemental Figure 2B), the latter of which is demonstrated to induce an alternative macrophage phenotype.[21]

Plaque macrophages are thought to originate from circulating monocytes which are mobilized from bone marrow and spleen.[22,23] We therefore assessed potential changes in MC1-R expression in these organs and observed a drastic decrease in splenic MC1-R expression after 4 weeks of HFD followed by a partial recovery at 16 weeks HFD (Figure 2B). Bone marrow MC1-R expression showed an increasing trend in association with the duration of the HFD (Figure 2C), which might be explained by enhanced myelopoiesis and thus number of MC1-R expressing monocytes due to the hypercholesterolemia.

The aortic MC1-R gene expression pattern was further supported by immunofluorescence, which showed the strongest MC1-R staining in the lesions of 4 weeks HFD mice colocalizing in macrophage-rich areas (Figure 2D). In line with the human data, MC1-R expression was directly associated with ABCA1 and ABCG1 mRNA levels in the aorta of 4 weeks HFD mice (Figure 2E and 2F), while no significant association to SR-BI (Figure 2G), CD36 or SR-A (data not shown) was observed.

The Endogenous MC1-R Agonist α-MSH Inhibits Cholesterol Uptake and Increases Cholesterol Efflux in Macrophages

Given the association of MC1-R expression with regulators of reverse cholesterol transport, we further aimed to investigate the role of MC1-R in macrophage cholesterol metabolism. To this end, we loaded BMDMs with [3H]-cholesterol prior to treatment with the natural MC1-R agonist α-MSH in order to measure cholesterol efflux onto the lipid acceptors ApoA1 or HDL. We found that α-MSH significantly increased efflux capacity to HDL without affecting cholesterol efflux to ApoA1 (Figure 3A), potentially reflecting an alteration in ABCG1 or SR-BI expression. As an additional protective mechanism against foam cell formation, α-MSH reduced the uptake of oxLDL after a short-term treatment but failed to sustain this effect when the oxLDL loading was performed after 24h of α-MSH stimulation (Figure 3B). To address the molecular mechanisms behind these effects, we quantified the protein levels of key mediators of cholesterol efflux (ABCA1, ABCG1 and SR-BI) and uptake (CD36 and SR-A) after 24h treatment with α-MSH. Consistent with the functional efflux data, α-MSH increased ABCG1 protein levels and caused a biphasic response in ABCA1 expression with declining levels after high concentrations of α-MSH (Figure 3C and Supplemental Figure 3A). α-MSH also elevated CD36 expression (Figure 3C and Supplemental Figure 3A), which accounts for ~50% of cholesterol uptake in macrophages and therefore contradicts the finding of reduced oxLDL uptake in α-MSH-treated macrophages. To clarify this discrepancy, we determined cell surface expression of CD36 by flow cytometry after acute α-MSH stimulation and found that α-MSH markedly

reduced membrane-associated CD36 (Figure 3D and E), thereby also interfering with oxLDL-induced internalization of CD36 (Figure 3F). This effect was lost after 24h stimulation with α-MSH (Supplemental Figure 3B). Despite the increase of total CD36 expression, observed by Western blotting, oxLDL uptake was not augmented by α-MSH, indicating that the effect on CD36 surface expression is the dominant factor determining cholesterol uptake of α-MSH-treated macrophages. Since SR-BI level has an inverse relationship with cellular cholesterol pools,[24] we loaded BMDMs with oxLDL and assayed them for SR-BI to further investigate whether α-MSH is capable of preventing cholesterol accumulation. Of note, α-MSH attenuated oxLDL-induced reduction of SR-BI (Figure 3G). Finally, since ABCA1 and ABCG1 transporters have been reported to control leukocytosis,[25,26] we assessed the proliferation rate of α-MSH-treated BMDMs, revealing that the amount of cells in active G1 phase was reduced by α-MSH (Figure 3I and IJ). Collectively, these results indicate that α-MSH enhances cholesterol efflux onto HDL and inhibits CD36-mediated lipid uptake in macrophages while limiting macrophage proliferation.

Selective MC1-R Agonists Mimic the Effects of α-MSH

Since the natural ligand α-MSH does not only bind to MC1-R, we next tested whether selective MC1-R agonists evoke similar effects in BMDMs. We used LD211 and MSG606, which have been shown to have high affinity for MC1-R with no or only minimal binding to other MC-R subtypes.[16,27] In BMDMs, LD211 acted like a classical agonist causing a strong response in cAMP assay, while MSG606 reduced intracellular cAMP concentration, a characteristic of an inverse agonist (Supplemental Figure 4A and 4B). Furthermore, both agonists were able to engage other signaling cascades, namely phosphorylation of extracellular signal–regulated kinase (ERK1/2) and dephosporylation of p38 MAP kinase, in a time- and dose-dependent manner (Supplemental Figure 4C–4F). Of note, MSG606 had a stronger effect on ERK1/2 phosphorylation compared to LD211 (Supplemental Figure 4E). In terms of the signaling responses, the maximal effects were reached in the micromolar range. We therefore used micromolar concentrations of these compounds for subsequent experiments.

First, we characterized the potential anti-inflammatory effects of these compounds in LPS-stimulated BMDMs. LD211 showed only modest suppression of cytokine mRNA expression and secretion with preferential effects on IL-6 and CCL2 (Supplemental Figure 5). MSG606 caused somewhat divergent effects and selectively reduced the mRNA expression of IL-1β and TNFα (Supplemental Figure 6). Overall, the anti-inflammatory effects of the agonists were weak and comparable to those of α-MSH.

Second, the effects on cholesterol transporter proteins were investigated, demonstrating that the selective MC1-R agonists, like α-MSH, increase ABCA1 and ABCG1 protein levels (Figure 4A). MSG606 showed no other effects, while LD211 caused reductions in SR-BI and SR-A levels and an increase in CD36 expression (Figure 4A). To investigate the mechanism behind increased ABCA1 and ABCG1 protein, we first quantified mRNA expression and found that both compounds upregulated ABCA1 and ABCG1 without affecting liver X receptor alpha (LXRα), which is one of the strongest inducers of ABCA1

and ABCG1 (Figure 4C). We also assessed whether MC1-R activation regulates the expression of other LXRα target genes such as ApoE. Both agonists were devoid of a systemic effect on the analyzed target genes, except for cholesterol 7 alpha-hydoxylase (CYP7A1) (Supplemental Figure 7), which was specifically upregulated upon treatment. CYP7A1 is involved in cholesterol catabolism and might help macrophages to maintain cholesterol homeostasis.[28]

Since ABCA1 and ABCG1 expression is strongly regulated by diverse posttranscriptional mechanisms, we conducted additional experiments to determine whether MC1-R activation influences mRNA or protein stability of these transporters. Blocking transcription with actinomycin D revealed that mRNA stability of ABCA1 and ABCG1 was unchanged after 4h (data not shown) or 24h treatment with LD211 or MSG606 (Supplemental Figure 8). Furthermore, these compounds did not increase the stability of ABCA1 protein (Supplemental Figure 9). Given that miRNAs have recently emerged as critical regulators of ABCA1 and ABCG1,[29,30] we next explored whether MC1-R activation modulates the expression of miRNAs that are known to target and repress these transporters. However, LD211 and MSG606 had no consistent effects on the expression of miRNAs such as miR-33, miR-148a or miR-758 (Supplemental Figure 10), excluding the possibility that miRNAs are primarily driving the observed effects. Taken together, the data suggest that the upregulation of ABCA1 and ABCG1 protein is mainly attributable to transcriptional induction.

Importantly, the upregulation of ABCA1 and ABCG1 transporters translated functionally into enhanced cholesterol efflux to both ApoA1 and HDL (Figure 4D). In line with the effects of α-MSH, selective agonism of MC1-R acutely reduced the cell surface expression of CD36 as well as attenuated cholesterol uptake (Figure 4E and 4F). BMDMs were also loaded with oxLDL and then quantified for LXRα expression as a sensitive marker of cholesterol influx. LD211 and MSG606 effectively attenuated the oxLDL-induced increase in LXRα expression (Figure 4G). Similarly to α-MSH, these compounds were able to restore the SR-BI levels in the oxLDL-loaded state (Figure 4H and 4I), further evidencing that MC1-R activation prevents lipid accumulation. Proliferation of BMDMs was also reduced by treatment with MSG606 but not with LD211 (Figure 4J). These data suggest that MC1-R is responsible for the observed effects of α-MSH on macrophage cholesterol transport.

Macrophages Deficient in Functional MC1-R Display Enhanced Cholesterol Uptake and Reduced Efflux Capacity

To investigate whether loss-of-function of MC1-R in macrophages translates into a reverse phenotype compared to MC1-R activation, we isolated BMDMs from mice deficient in functional MC1-R signaling (MC1-R$^{e/e}$) and their WT littermates and determined first the cholesterol accumulation in these cells. Indeed, MC1-R$^{e/e}$ macrophages showed increased uptake of Dil-oxLDL (Figure 5A) as well as higher proportion of Oil-Red-O positive cells after oxLDL loading (Figure 5B). At the molecular level, MC1-R$^{e/e}$ BMDMs had an augmented LXRα expression in response to oxLDL (Figure 5C). In agreement with increased cholesterol uptake, we observed higher cell-surface and mRNA levels of CD36 in

MC1-R$^{e/e}$ macrophages (Figure 5D and 5F). Functionally, MC1-R deficient BMDMs also displayed reduced cholesterol efflux onto ApoA1 and HDL compared to WT BMDMs (Figure 5E). Consistent with the reduced efflux onto ApoA1, ABCA1 mRNA expression was lower in MC1-R$^{e/e}$ macrophages (Figure 5F). Gene expression data also showed less SR-BI but unchanged ABCG1 levels in MC1-R$^{e/e}$ (Figure 5F). However, Western blot analysis revealed reduced ABCG1 protein expression under baseline conditions, which might partly account for the impaired efflux rate onto HDL (Figure 5G and 5H).

In addition to cholesterol metabolism, we determined the expression of pro- and anti-inflammatory markers in MC1-R$^{e/e}$ macrophages under baseline and stimulated conditions. Unexpectedly, deficient MC1-R signaling was associated with reduced mRNA levels of pro-inflammatory M1 markers IL-1β and TNFα in unstimulated conditions as well as with suppressed IL-1β and IL-6 response to LPS (Supplemental Figure 11). However, ELISA analysis revealed that release of these cytokines was unaltered in MC1-R$^{e/e}$ BMDMs (Supplemental Figure 11), reflecting potentially a difference in mRNA stability. Anti-inflammatory M2 markers, arginase-1 and C-C motif chemokine 22, were also reduced in unstimulated MC1-R$^{e/e}$ BMDMs, while IL-4-induced upregulation of the M2 markers was not compromised in these cells (Supplemental Figure 11). Taken together, macrophages deficient in functional MC1-R showed increased propensity for foam cell formation with no evident inflammatory phenotype.

Targeting of MC1-R *in vivo* Improves Plaque Stability but Does not Reduce Lesion Size in Atherosclerotic ApoE$^{-/-}$ Mice

In order to validate the *in vivo* relevance of MC1-R in macrophage cholesterol metabolism, we subjected ApoE$^{-/-}$ mice to daily injections of the MC1R agonist MSG606 (1mg/kg/day) in parallel to 4 weeks HFD. The prominent MC1-R expression within atherosclerotic plaques after 4wks of HFD prompted us to therapeutically target this early phase of plaque development. Chronic treatment of ApoE$^{-/-}$ mice with MSG606 had no effect on body weight gain (data not shown), but it significantly reduced total cholesterol levels in the plasma compared to the control group (Figure 6A). This reduction was evenly distributed in the VLDL and LDL fractions (Figure 6B), which retain ~95% of the total plasma cholesterol in ApoE$^{-/-}$ mice. The total plaque area at the level of the aortic sinus and lesional macrophage coverage as judged by relative Mac-2-positive area of aortic root sections were not affected by MSG606 (Figure 6C–6E). However, gene expression analysis of aortic lysates revealed significantly reduced CD36 mRNA levels in MSG606-treated mice as well as increased the expression of collagen (Col1A2 and Col3A1) and α-smooth muscle actin (αSMA), which are markers of plaque stability (Figure 6F and 6G). Masson's trichrome staining of aortic root sections further evidenced higher collagen content in the lesions of MSG606-treated mice (Figure 6H and 6I). Since the gene expression analysis of whole aortas did not reveal significant changes of ABCG1 mRNA levels, we further aimed to quantify ABCG1 expression specifically in plaque macrophages by double immunofluorescence. Indeed, we found more pronounced ABCG1 staining in mice colocalizing with plaque macrophages (Figure 6J and 6K), thereby extending our *in vitro* findings on reverse cholesterol transporters into an *in vivo* setting.

To investigate other contributing factors for the reduced plasma cholesterol, we first analyzed the expression of cholesterol transport and synthesis genes in the liver. MSG606 treatment increased hepatic ABCA1 and ABCG1 as well as LDL receptor mRNA levels without affecting the expression of cholesterol synthesis genes (Supplemental Figure 12). Importantly, MSG606 treatment did not aggravate lipid accumulation in the liver (Supplemental Figure 12). Further profiling of gene expression revealed that CD36 was downregulated in the spleen, while the analysis of bone marrow samples revealed no significant effects (Supplemental Figure 13). In addition, cytokine levels were unaltered in the plasma of MSG606-treated mice (Supplemental Figure 13).

We also performed flow cytometry analyses of the aorta, blood, spleen and bone marrow of treated ApoE$^{-/-}$ mice to assess potential differences in leukocyte subsets (Figure 7A). Despite that Mac-2 immunohistochemistry revealed no signs of treatment effect, MSG606-treated mice had less Ly6C^{high} monocytes in the aorta (Figure 7B), while circulating monocyte counts were higher (Figure 7C–7E). We may speculate that the decrease in Ly6C^{high} monocyte counts in aortas of MSG606-treated mice might be due to enhanced mobilization or reduced recruitment to the plaque, which might also reflect the higher circulating monocyte counts. To clarify this, we conducted *in vitro* experiments with endothelial cells and found that MSG606 treatment reduced VCAM-1, IL-6 and CCL2 mRNA expression of TNFα-stimulated cells (Supplemental Figure 14). Finally, flow cytometric analysis of spleen and bone marrow did not reveal any significant effects of MSG606 on leukocyte subsets or progenitors (Supplemental Figure 15), arguing against a possible induction of myelopoiesis. Likewise, hematopoietic stem cells in the bone marrow, whose proliferation is partly controlled by ABCA1 and ABCG1 expression, were unaffected by MSG606 (Supplemental Figure 15).

DISCUSSION

Several lines of evidence indicate that MC1-R activation in macrophages is functionally linked to anti-inflammatory modulation and proresolving properties,[1] but the present findings unveil a completely new aspect of MC1-R biology. A series of *in vitro* experiments demonstrated that triggering MC1-R signaling either with its natural ligand α-MSH or synthetic MC1-R agonists protects macrophages against excessive cholesterol accumulation and foam cell formation. This finding is likely explained by two main factors. First, MC1-R activation down-regulated the expression of cell surface CD36, which belongs to the scavenger receptor family and interacts with multiple ligands including oxLDL.[31] Given that CD36 significantly contributes to foam cell formation and promotes atherosclerosis,[31,32] the inhibition of CD36-mediated oxLDL uptake by MC1-R is likely to be atheroprotective. The exact molecular mechanism for CD36 downregulation upon MC1-R activation is unknown but it is driven by a cAMP-independent signaling cascade, since MSG606 evoked a similar response to α-MSH. Second, we identified that MC1-R activation strongly enhances cholesterol efflux onto both ApoA1 and HDL through LXRα-independent upregulation of ABCA1 and ABCG1 expression. The effects of α-MSH and selective MC1-R agonists were for the most part consistent except for small differences such as the lack of effect of α-MSH on ABCA1-mediated cholesterol efflux. In the case of α-MSH, the interpretation of the results is complicated by its agonistic activity at MC3-R, which is abundantly expressed by

macrophages.[9] Furthermore, α-MSH is naturally produced and released by macrophages and thereby, treating cells with supraphysiological concentrations of α-MSH might disturb the autocrine/paracrine signaling of the α-MSH/MC1-R-axis and lead to unexpected responses.[5,33]

In good agreement with our findings on MC1-R agonism, we found that dysfunctional MC1-R in macrophages was associated with a reverse phenotype, namely enhanced cholesterol uptake and disturbed efflux machinery. Surprisingly, MC1-R deficient macrophages were devoid of a pro-inflammatory phenotype, which was expected to appear based on the previous and present findings that stimulation of MC1-R exerts anti-inflammatory actions. On the other hand, we noted that cytokine expression was only modestly suppressed by MC1-R activation compared to the much stronger effects on cholesterol transport. These results are in line with a previous notion that MC1-R is not the dominant receptor subtype in mediating the anti-inflammatory actions of melanocortin peptides in murine macrophages.[7] In contrast, the present data clearly illustrate that MC1-R carries a non-redundant role in the regulation of cholesterol transport.

To further explore the concept of MC1-R-mediated regulation of cholesterol transport and its translation into therapeutic effectiveness *in vivo*, atherosclerotic ApoE$^{-/-}$ mice were chronically treated with MSG606. This compound was selected for *in vivo* testing mainly for two reasons. First, MSG606 showed superior potency to LD211 in terms of harnessing protective mechanisms against foam cell formation. Second, from a drug development perspective, biased agonism, that is pathway-selective, is an emerging concept with significant therapeutic interest.[34] We found that MSG606 acts like a biased agonist by promoting ERK, but not cAMP signaling. With this kind of compound, it is possible to target only the therapeutically important pathways and to avoid activating pathways that lead to side effects. In the case of MC1-R biology, melanogenesis is evoked by cAMP formation and thereby dissociating this pathway prevents the unwanted pigmentary effects. Biased agonism of MC1- and MC3-R with a small molecule, AP1189, has been recently proven to be a viable approach for suppressing inflammation in conditions like peritonitis and arthritis.[35] Here, we were able to further validate this concept and to prove its applicability in a different biological context.

By targeting MC1-R for the treatment of atherosclerosis, we aimed to build on the paradigm that efficient cholesterol efflux from macrophages, through maintained integrity of ABCA1 and ABCG1 transporters, is atheroprotective.[36] However, although strongly promoting cholesterol efflux in cultured BMDMs and showing similar responses at the molecular level *in vivo* combined with a cholesterol-lowering effect, MSG606 did not limit plaque size in ApoE$^{-/-}$ mice. This might be due to several reasons. Firstly, the pharmacokinetic properties of MSG606 have not been previously evaluated and hence, it is unknown whether the selected dose and frequency of drug administration were sufficient. Secondly, we observed that lesional MC1-R expression localized to a distinct and limited subset of macrophages, which raises the question whether activation of this restricted population is effective enough to confer protection against plaque development. Thirdly, previous studies using transgenic models of ABCA1 and ABCG1 overexpression on an ApoE$^{-/-}$ background have failed to demonstrate atheroprotective effects.[37,38] The absence of ApoE lowers the plasma levels of

ApoA1 and HDL and impairs cholesterol efflux from macrophages, which might neutralize the effectiveness of drugs that are acting on cholesterol efflux transporters. And finally, the atheroprotective effect linked to improved cholesterol metabolism might be more pronounced at more advanced plaque stage. Therefore, further experiments are warranted to determine whether modified dosing and treatment timing of the MSG606 therapy or alternative ways to target the MC1-R could eventually halt the development of atherosclerotic plaques or even lead to regression of existing plaques in a different atherosclerosis model. Nevertheless, MSG606 treatment promoted signs of plaque stability, indicating that it favorably tunes the balance between collagen synthesis and breakdown through a yet unknown mechanism. Furthermore, we found that MSG606 reduced arterial monocyte accumulation with a concomitant increase in circulating $Ly6C^{low}$ monocytes. It is noteworthy that these changes occurred without induction of myelopoiesis. The underlying mechanism for this is likely to be multifactorial, involving downregulation of adhesion molecule and cytokine expression both in monocytes and ECs. This notion is supported by previous findings demonstrating that MC1-R activation inhibits monocyte adhesion to inflamed vasculature.[39,40] Importantly, these results provide evidence that MC1-R activation *in vivo* promotes advantageous changes in plaque architecture.

In conclusion, our findings uncover a novel role for MC1-R in macrophage cholesterol transport, which is independent of cAMP signaling. Triggering MC1-R signaling in macrophages suppresses cholesterol uptake and promotes reverse cholesterol transport, which are preventive mechanisms against foam cell formation and the progression of atherosclerosis.

Supplementary Material

Refer to Web version on PubMed Central for supplementary material.

Acknowledgments

We thank Diana Wagner, Yvonne Jansen, Mauricio Velasco-Delgado, Elina Kahra and Marja-Riitta Kajaala for excellent technical assistance, and Eriika Savontaus for providing samples from $MC1\text{-}R^{e/e}$ mice.

Sources of Funding

This work was financially supported by the Academy of Finland (grant 274852 to P.R.), the Finnish Foundation for Cardiovascular Research (to P.R.), the Paavo Nurmi Foundation (to P.R.), the Alexander von Humboldt Foundation (to E.P.C.v.d.V.), the National Institutes of Health (grant GM-108040 to V.J.H. & M.C.), the Deutsche Forschungsgemeinschaft (STE-1053/3-1 to S.S. and as part of the SFB1123 TP A1 to C.W.), the Else Kroener Fresenius Foundation (2013_A114 to S.S.), the German Centre for Cardiovascular Research (DZHK MHA VD1.2 to C.W.), and the European Research Council ERC (AdG 249929 to C.W.). The Tampere Vascular Study has been financially supported by the Academy of Finland: grants 286284 (to T.L.), 285902 (to E.R.); Tampere University Hospital Medical Funds (grant X51001); Juho Vainio Foundation; Paavo Nurmi Foundation; Finnish Foundation for Cardiovascular Research; Finnish Cultural Foundation; Tampere Tuberculosis Foundation; Emil Aaltonen Foundation; Yrjö Jahnsson Foundation; and Signe and Ane Gyllenberg Foundation.

References

1. Catania A, Gatti S, Colombo G, Lipton JM. Targeting melanocortin receptors as a novel strategy to control inflammation. Pharmacol Rev. 2004; 56:1–29. [PubMed: 15001661]
2. Wikberg JE, Mutulis F. Targeting melanocortin receptors: an approach to treat weight disorders and sexual dysfunction. Nat Rev Drug Discov. 2008; 7:307–323. [PubMed: 18323849]

3. Mountjoy K, Robbins L, Mortrud M, Cone R. The cloning of a family of genes that encode the melanocortin receptors. Science. 1992; 257:1248–1251. [PubMed: 1325670]

4. Lerner AB, McGuire JS. Effect of alpha- and betamelanocyte stimulating hormones on the skin colour of man. Nature. 1961; 189:176–179. [PubMed: 13761067]

5. Star RA, Rajora N, Huang J, Stock RC, Catania A, Lipton JM. Evidence of autocrine modulation of macrophage nitric oxide synthase by alpha-melanocyte-stimulating hormone. Proc Natl Acad Sci U S A. 1995; 92:8016–8020. [PubMed: 7544012]

6. Bhardwaj R, Becher E, Mahnke K, Hartmeyer M, Schwarz T, Scholzen T, Luger TA. Evidence for the differential expression of the functional alpha-melanocyte-stimulating hormone receptor MC-1 on human monocytes. J Immunol. 1997; 158:3378–3384. [PubMed: 9120297]

7. Getting SJ, Christian HC, Lam CW, Gavins FN, Flower RJ, Schiöth HB, Perretti M. Redundancy of a functional melanocortin 1 receptor in the anti-inflammatory actions of melanocortin peptides: studies in the recessive yellow (e/e) mouse suggest an important role for melanocortin 3 receptor. J Immunol. 2003; 170:3323–3330. [PubMed: 12626592]

8. Böhm M, Luger TA, Steingräber AK, Goerge T. Is MC1 dispensable for regulation of cutaneous inflammatory and immune responses? Exp Dermatol. 2013; 22:792–794. [PubMed: 24131319]

9. Getting SJ, Gibbs L, Clark AJ, Flower RJ, Perretti M. POMC gene-derived peptides activate melanocortin type 3 receptor on murine macrophages, suppress cytokine release, and inhibit neutrophil migration in acute experimental inflammation. J Immunol. 1999; 162:7446–7453. [PubMed: 10358199]

10. Hansson GK, Libby P. The immune response in atherosclerosis: a double-edged sword. Nat Rev Immunol. 2006; 6:508–5019. [PubMed: 16778830]

11. Weber C, Noels H. Atherosclerosis: current pathogenesis and therapeutic options. Nat Med. 2011; 17:1410–1422. [PubMed: 22064431]

12. Moore KJ, Sheedy FJ, Fisher EA. Macrophages in atherosclerosis: a dynamic balance. Nat Rev Immunol. 2013; 13:709–721. [PubMed: 23995626]

13. Hilgendorf I, Swirski FK, Robbins CS. Monocyte fate in atherosclerosis. Arterioscler Thromb Vasc Biol. 2015; 35:272–279. [PubMed: 25538208]

14. Moore KJ, Tabas I. Macrophages in the pathogenesis of atherosclerosis. Cell. 2011; 145:341–355. [PubMed: 21529710]

15. Tall AR, Yvan-Charvet L. Cholesterol, inflammation and innate immunity. Nat Rev Immunol. 2015; 15:104–116. [PubMed: 25614320]

16. Cai M, Stankova M, Muthu D, Mayorov A, Yang Z, Trivedi D, Cabello C, Hruby VJ. An unusual conformation of γ-melanocyte-stimulating hormone analogues leads to a selective human melanocortin 1 receptor antagonist for targeting melanoma cells. Biochemistry. 2013; 52:752–764. [PubMed: 23276279]

17. Levula M, Airla N, Oksala N, Hernesniemi JA, Pelto-Huikko M, Salenius JP, Zeitlin R, Järvinen O, Huovila AP, Nikkari ST, Jaakkola O, Ilveskoski E, Mikkelsson J, Perola M, Laaksonen R, Kytömäki L, Soini JT, Kähönen M, Parkkinen J, Karhunen PJ, Lehtimäki T. ADAM8 and its single nucleotide polymorphism 2662 T/G are associated with advanced atherosclerosis and fatal myocardial infarction: Tampere vascular study. Ann Med. 2009; 41:497–507. [PubMed: 19575316]

18. Oksala N, Pärssinen J, Seppälä I, Raitoharju E, Kholova I, Ivana K, Hernesniemi J, Lyytikäinen LP, Levula M, Mäkelä KM, Sioris T, Kähönen M, Laaksonen R, Hytönen V, Lehtimäki T. Association of neuroimmune guidance cue netrin-1 and its chemorepulsive receptor UNC5B with atherosclerotic plaque expression signatures and stability in human(s): Tampere Vascular Study (TVS). Circ Cardiovasc Genet. 2013; 6:579–587. [PubMed: 24122613]

19. Raitoharju E, Seppälä I, Lyytikäinen LP, Levula M, Oksala N, Klopp N, Illig T, Laaksonen R, Kähönen M, Lehtimäki T. A comparison of the accuracy of Illumina HumanHT-12 v3 Expression BeadChip and TaqMan qRT-PCR gene expression results in patient samples from the Tampere Vascular Study. Atherosclerosis. 2013; 226:149–152. [PubMed: 23177970]

20. Rinne P, Ahola-Olli A, Nuutinen S, Koskinen E, Kaipio K, Eerola K, Juonala M, Kähönen M, Lehtimäki T, Raitakari OT, Savontaus E. Deficiency in Melanocortin 1 Receptor Signaling

Predisposes to Vascular Endothelial Dysfunction and Increased Arterial Stiffness in Mice and Humans. Arterioscler Thromb Vasc Biol. 2015; 35:1678–1686. [PubMed: 25931512]

21. Rios FJ, Koga MM, Pecenin M, Ferracini M, Gidlund M, Jancar S. Oxidized LDL induces alternative macrophage phenotype through activation of CD36 and PAFR. Mediators Inflamm. 2013; 2013:198193. [PubMed: 24062612]
22. Swirski FK, Pittet MJ, Kircher MF, Aikawa E, Jaffer FA, Libby P, Weissleder R. Monocyte accumulation in mouse atherogenesis is progressive and proportional to extent of disease. Proc Natl Acad Sci U S A. 2006; 103:10340–10345. [PubMed: 16801531]
23. Robbins CS, Chudnovskiy A, Rauch PJ, Figueiredo JL, Iwamoto Y, Gorbatov R, Etzrodt M, Weber GF, Ueno T, van Rooijen N, Mulligan-Kehoe MJ, Libby P, Nahrendorf M, Pittet MJ, Weissleder R, Swirski FK. Extramedullary hematopoiesis generates Ly-6C(high) monocytes that infiltrate atherosclerotic lesions. Circulation. 2012; 125:364–374. [PubMed: 22144566]
24. Han J, Nicholson AC, Zhou X, Feng J, Gotto AM, Hajjar DP. Oxidized low density lipoprotein decreases macrophage expression of scavenger receptor B-I. J Biol Chem. 2001; 276:16567–16572. [PubMed: 11278882]
25. Yvan-Charvet L, Ranalletta M, Wang N, Han S, Terasaka N, Li R, Welch C, Tall AR. Combined deficiency of ABCA1 and ABCG1 promotes foam cell accumulation and accelerates atherosclerosis in mice. J Clin Invest. 2007; 117:3900–3908. [PubMed: 17992262]
26. Out R, Hoekstra M, Habets K, Meurs I, de Waard V, Hildebrand RB, Wang Y, Chimini G, Kuiper J, Van Berkel TJ, Van Eck M. Combined deletion of macrophage ABCA1 and ABCG1 leads to massive lipid accumulation in tissue macrophages and distinct atherosclerosis at relatively low plasma cholesterol levels. Arterioscler Thromb Vasc Biol. 2008; 28:258–264. [PubMed: 18006857]
27. Doedens L, Opperer F, Cai M, Beck JG, Dedek M, Palmer E, Hruby VJ, Kessler H. Multiple N-methylation of MT-II backbone amide bonds leads to melanocortin receptor subtype hMC1R selectivity: pharmacological and conformational studies. J Am Chem Soc. 2010; 132:8115–8128. [PubMed: 20496895]
28. Russell DW. Nuclear orphan receptors control cholesterol catabolism. Cell. 1999; 97:539–542. [PubMed: 10367881]
29. Canfrán-Duque A, Ramírez CM, Goedeke L, Lin CS, Fernández-Hernando C. microRNAs and HDL life cycle. Cardiovasc Res. 2014; 103:414–422. [PubMed: 24895349]
30. Rotllan N, Price N, Pati P, Goedeke L, Fernández-Hernando C. microRNAs in lipoprotein metabolism and cardiometabolic disorders. Atherosclerosis. 2016; 246:352–360. [PubMed: 26828754]
31. Park YM. CD36, a scavenger receptor implicated in atherosclerosis. Exp Mol Med. 2014; 46:e99. [PubMed: 24903227]
32. Febbraio M, Podrez EA, Smith JD, Hajjar DP, Hazen SL, Hoff HF, Sharma K, Silverstein RL. Targeted disruption of the class B scavenger receptor CD36 protects against atherosclerotic lesion development in mice. J Clin Invest. 2000; 105:1049–1056. [PubMed: 10772649]
33. Rajora N, Ceriani G, Catania A, Star RA, Murphy MT, Lipton JM. alpha-MSH production, receptors, and influence on neopterin in a human monocyte/macrophage cell line. J Leukoc Biol. 1996; 59:248–253. [PubMed: 8603997]
34. Kenakin T, Christopoulos A. Signalling bias in new drug discovery: detection, quantification and therapeutic impact. Nat Rev Drug Discov. 2013; 12:205–216. [PubMed: 23411724]
35. Montero-Melendez T, Gobbetti T, Cooray SN, Jonassen TE, Perretti M. Biased agonism as a novel strategy to harness the proresolving properties of melanocortin receptors without eliciting melanogenic effects. J Immunol. 2015; 194:3381–3388. [PubMed: 25725103]
36. Rosenson RS, Brewer HB, Davidson WS, Fayad ZA, Fuster V, Goldstein J, Hellerstein M, Jiang XC, Phillips MC, Rader DJ, Remaley AT, Rothblat GH, Tall AR, Yvan-Charvet L. Cholesterol efflux and atheroprotection: advancing the concept of reverse cholesterol transport. Circulation. 2012; 125:1905–1919. [PubMed: 22508840]
37. Joyce CW, Amar MJ, Lambert G, Vaisman BL, Paigen B, Najib-Fruchart J, Hoyt RF, Neufeld ED, Remaley AT, Fredrickson DS, Brewer HB, Santamarina-Fojo S. The ATP binding cassette

transporter A1 (ABCA1) modulates the development of aortic atherosclerosis in C57BL/6 and apoE-knockout mice. Proc Natl Acad Sci U S A. 2002; 99:407–412. [PubMed: 11752403]

38. Burgess B, Naus K, Chan J, Hirsch-Reinshagen V, Tansley G, Matzke L, Chan B, Wilkinson A, Fan J, Donkin J, Balik D, Tanaka T, Ou G, Dyer R, Innis S, McManus B, Lütjohann D, Wellington C. Overexpression of human ABCG1 does not affect atherosclerosis in fat-fed ApoE-deficient mice. Arterioscler Thromb Vasc Biol. 2008; 28:1731–1737. [PubMed: 18599800]
39. Yang Y, Zhang W, Meng L, Yu H, Lu N, Fu G, Zheng Y. Alpha-melanocyte stimulating hormone inhibits monocytes adhesion to vascular endothelium. Exp Biol Med (Maywood). 2015; 240:1537–1542. [PubMed: 25898835]
40. Leoni G, Voisin MB, Carlson K, Getting S, Nourshargh S, Perretti M. The melanocortin MC(1) receptor agonist BMS-470539 inhibits leucocyte trafficking in the inflamed vasculature. Br J Pharmacol. 2010; 160:171–180. [PubMed: 20331604]

CLINICAL PERSPECTIVE

What is new?

- Although the expression of melanocortin 1 receptor (MC1-R) and its role in modulating inflammatory responses in macrophages have been previously established, we here identify a novel regulatory function for MC1-R in macrophage cholesterol transport.
- Activation of macrophage MC1-R promotes the clearance of excess cholesterol from macrophages by increasing the expression ATP-binding cassette transporters ABCA1 and ABCG1, which initiate macrophage reverse cholesterol transport (RCT).
- Moreover, MC1-R signaling inhibits the uptake of oxidized low-density lipoprotein (oxLDL).
- *In vivo*, MC1-R expression localizes in atherosclerotic plaque macrophages and correlates with the levels of ABCA1 and ABCG1 transporters.

What are the clinical implications?

- The removal of excess cholesterol from macrophage-derived foam cells in atherosclerotic plaques is the critical first step of RCT, which facilitates the transport of peripheral cholesterol to the liver for excretion.
- Promoting macrophage RCT limits the progression of atherosclerosis and may ideally complement other lipid-lowering therapies to control for the residual risk that is often present in medically treated patients with atherosclerotic disease.
- Therefore, the identification of MC1-R in lesional macrophages and its role in regulating RCT, combined with the established anti-inflammatory effects of MC1-R, could serve as an attractive new approach for preventing atherosclerosis.

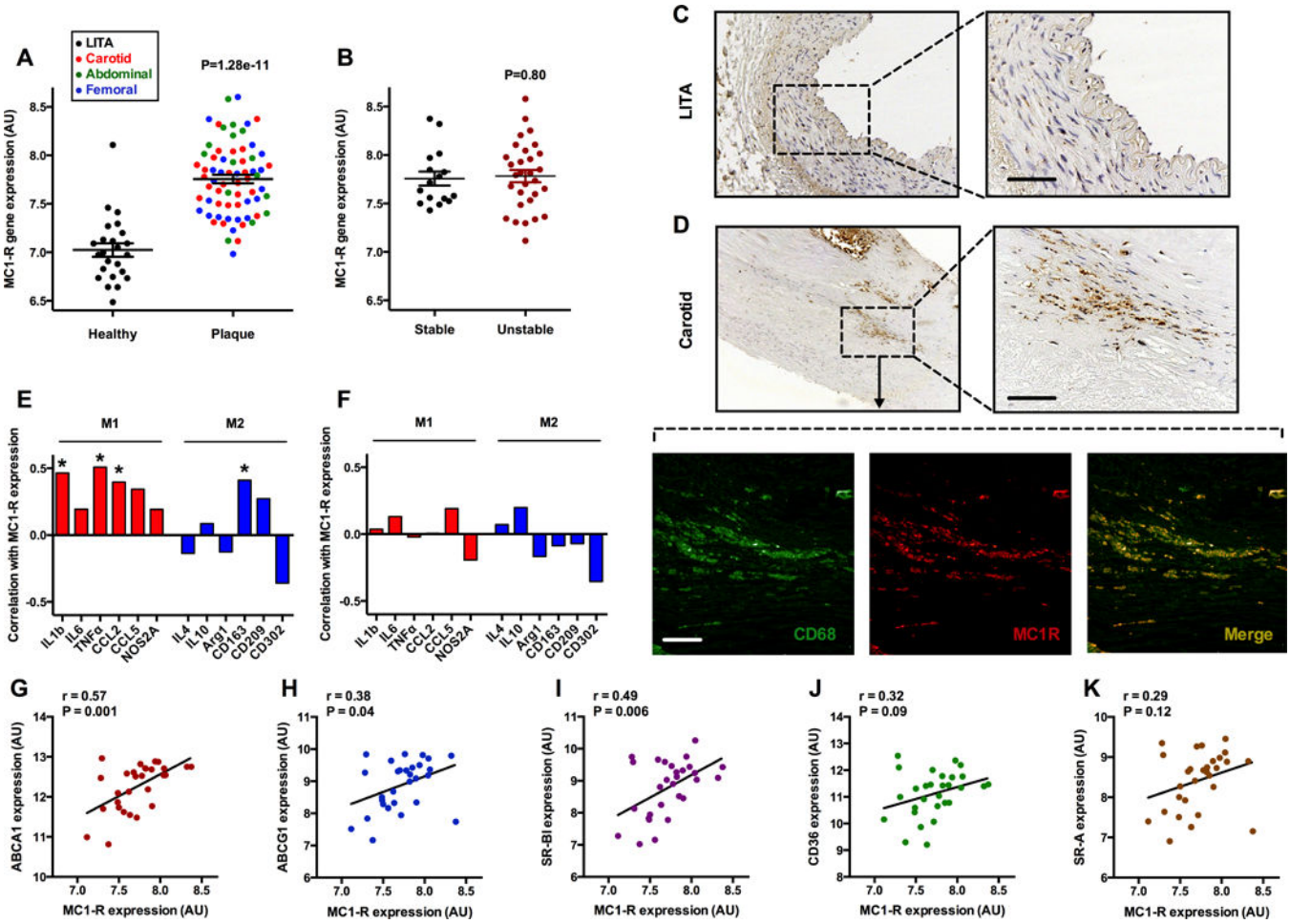

Figure 1. Melanocortin 1 receptor (MC1-R) is expressed by plaque macrophages in human atheroma

A, MC1-R expression in atherosclerosis-free control arteries (left internal thoracic artery; LITA) and in endarterectomy samples from the carotid artery, abdominal aorta and femoral artery. **B**, MC1-R expression in stable and unstable plaque phenotypes in a subgroup of advanced plaques (stage V and VI). Exact P-values are given in the graphs. MC1-R immunostaining of LITA (**C**) and carotid endarterectomy (**D**) samples. Scale bar, 25μm. A consecutive section of the carotid sample was immunofluorescently stained for MC1-R and CD68. Scale bar, 25μm. Correlation between MC1-R expression and established M1/M2 macrophage markers in carotid (**E**) and femoral (**F**) endarterectomy samples. Correlation coefficients (r) and statistical significances (* P<0.05) without correction for multiple comparisons are shown in the graphs. After false discovery rate (FDR) adjustment (q=0.05), correlation of MC1-R with TNFα remained significant. **G** through **K**, Correlations between MC1-R expression and ATP-binding cassette transporter A1 (ABCA1), G1 (ABCG1), scavenger receptor class B member 1 (SR-BI), CD36 or type 1 scavenger receptor class A (SR-A) expression in the carotid endarterectomy samples. Pearson correlation coefficients (r) and P values are presented in the graphs.

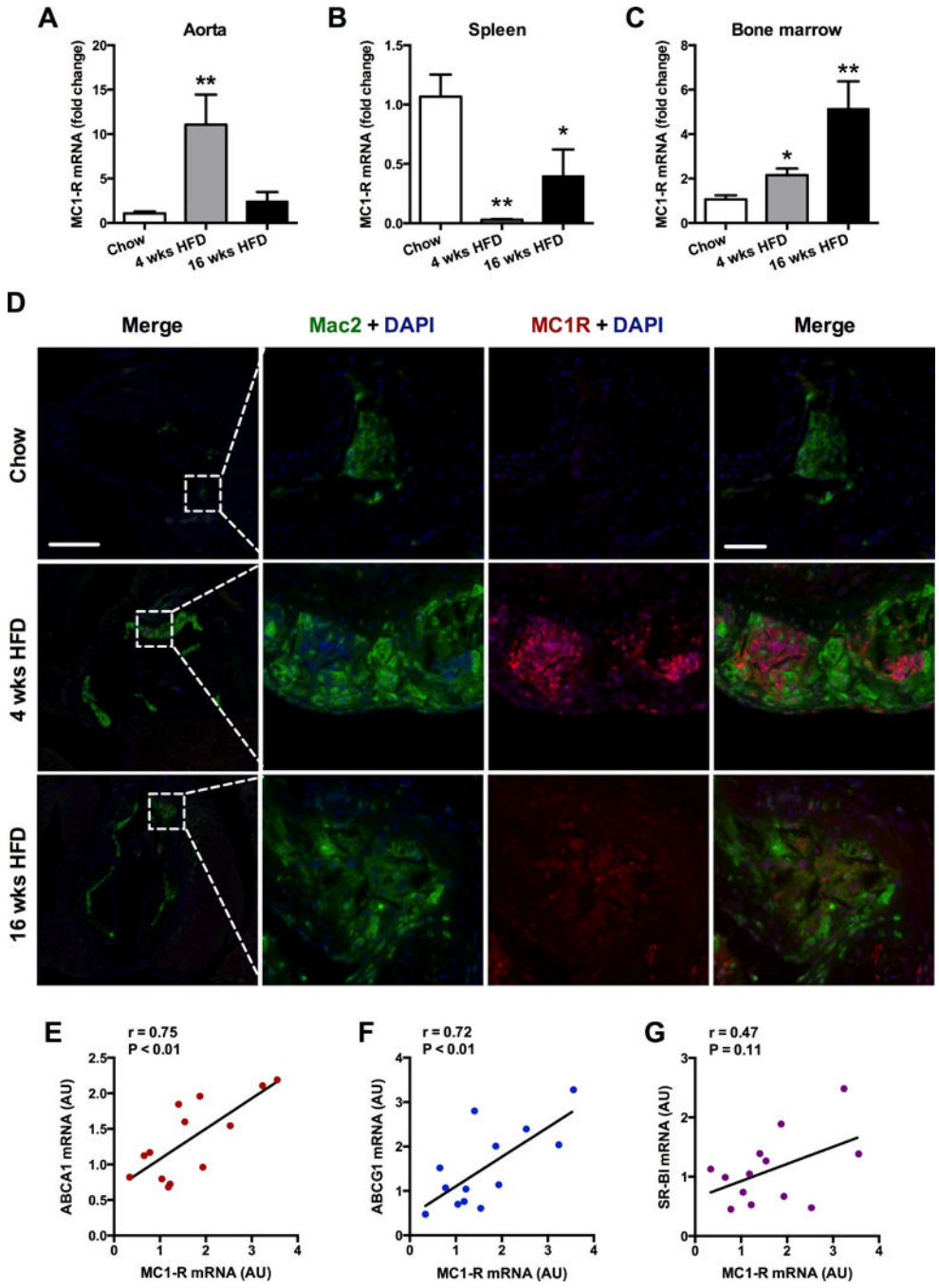

Figure 2. MC1-R expression in atherosclerotic ApoE$^{-/-}$ mice

Quantitative RT-PCR analysis of MC1-R expression in the aorta (**A**), spleen (**B**) and bone marrow (**C**) of ApoE$^{-/-}$ mice fed either a normal chow diet or high-fat diet (HFD). Data are expressed as mean ± SEM. * P<0.05 and ** P<0.01 versus chow, n=5 mice per group. **D**, Immunofluorescence of aortic root sections demonstrating staining for MC1-R in Mac-2^{+} intimal macrophages. Sections were obtained from ApoE$^{-/-}$ mice at different stages of plaque development. Scale bars, 500μm (left panel) and 50μm (right panel). Correlations between MC1-R gene expression and ABCA1 (**E**), ABCG1 (**F**) and SR-BI (**G**) gene

expression in the aorta of 4 wks HFD ApoE$^{-/-}$ mice. Pearson correlation coefficients (r) and P values are presented in the graphs.

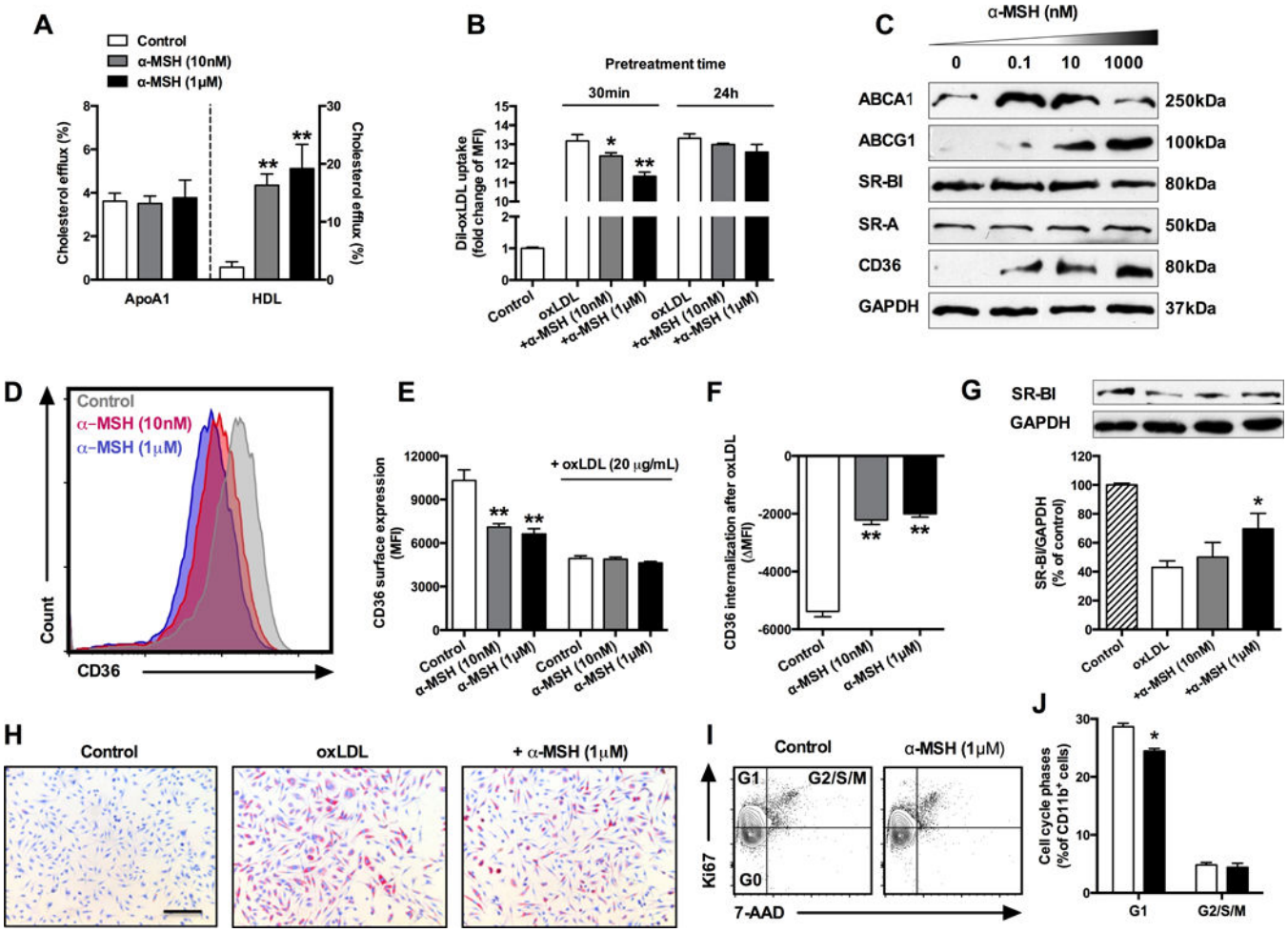

Figure 3. α-Melanocyte-stimulating hormone (α-MSH) reduces cholesterol uptake and enhances cholesterol efflux of macrophages

A, Cholesterol efflux onto apolipoprotein A1 (ApoA1) or high-density lipoprotein (HDL) in BMDMs stimulated with α-MSH. **B**, Flow cytometric analysis of Dil-conjugated oxLDL (Dil-oxLDL) uptake in α-MSH-treated BMDMs. Cells were treated with the indicated concentrations of α-MSH for 30min or 24h prior to loading them with Dil-oxLDL (10μg/mL) for 4h. **C**, Representative Western blots for ABCA1, ABCG1, SR-BI, SR-A, CD36 and glyceraldehyde 3-phosphate dehydrogenase (GAPDH; loading control) in BMDMs treated with increasing concentrations of α-MSH for 24h**. D**, Representative histograms for CD36 fluorescence intensity of control and α-MSH-treated BMDMs. **E**, Quantification of CD36 surface expression by flow cytometry in BMDMs treated with α-MSH for 30min followed by a 4h incubation in the absence or presence of oxLDL (20μg/mL). **F**, Change in CD36 surface expression after oxLDL loading (20μg/mL, 4h). **G**, Western blot analysis of SR-BI in control and oxLDL (20μg/mL, 24h) loaded BMDMs concomitantly treated with α-MSH. **H**, Oil-Red-O staining of untreated and oxLDL-treated (50μg/mL, 24h) BMDMs alone or in combination with α-MSH. Scale bar, 50μm. **I**, Representative dot plots with quadrants to identify BMDMs in G0 (lower left), G1 (upper left), and G2/S/M (upper right) phase after staining with Ki67 and 7-AAD. **J**, Quantification

of cells in G1 or G2/S/M phase after 24h treatment with α-MSH. * P<0.05 and ** P<0.01 versus control/oxLDL. Data are mean ± SEM, n=3–4 per group in each graph.

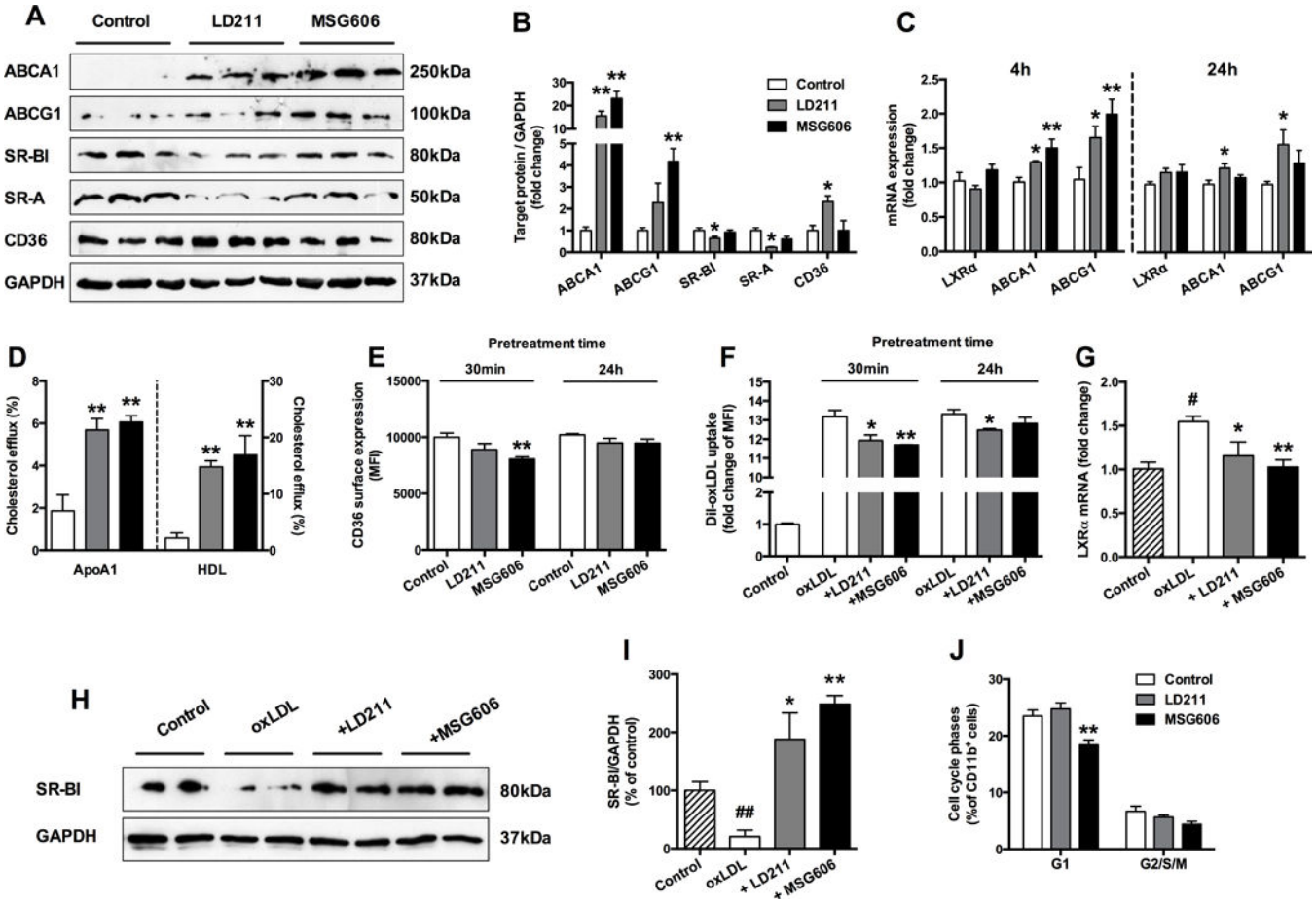

Figure 4. Selective agonism of MC1-R recapitulates the features of α-MSH treatment

A and **B**, Representative Western blots and quantification of ABCA1, ABCG1, SR-BI, SR-A, CD36 and GAPDH (loading control) in BMDMs treated with LD211 (1μM) or MSG606 (1μM) for 24h. **C**, Quantitative RT-PCR analysis of liver X receptor alpha (LXRα), ABCA1 and ABCG1 mRNA expression in BMDMs after 4h or 24h treatment with LD211 (1μM) or MSG606 (1μM). **D**, Cholesterol efflux onto ApoA1 or HDL in BMDMs treated with the MC1-R agonists. **E**, CD36 surface expression of BMDMs after 30min or 24h treatment with LD211 or MSG606. **F**, Dil-oxLDL uptake in BMDMs. Cells were treated with LD211 or MSG606 for 30min or 24h prior to loading them with Dil-oxLDL (10μg/mL) for 4h. **G**, Induction of LXRα mRNA expression after oxLDL (20μg/mL, 4h) treatment of BMDMs. The cells were left untreated or stimulated with LD211 or MSG606 for 30 min before oxLDL loading. **H** and **I**, Western blot analysis of SR-BI in control and oxLDL (20μg/mL, 24h) loaded BMDMs concomitantly treated with the MC1-R agonists. **J**, Quantification of cells in G1 or G2/S/M phase after 24h treatment with the MC1-R agonists. * P<0.05 and ** P<0.01 versus control/oxLDL. Data are mean ± SEM, 3–4 per group in each graph.

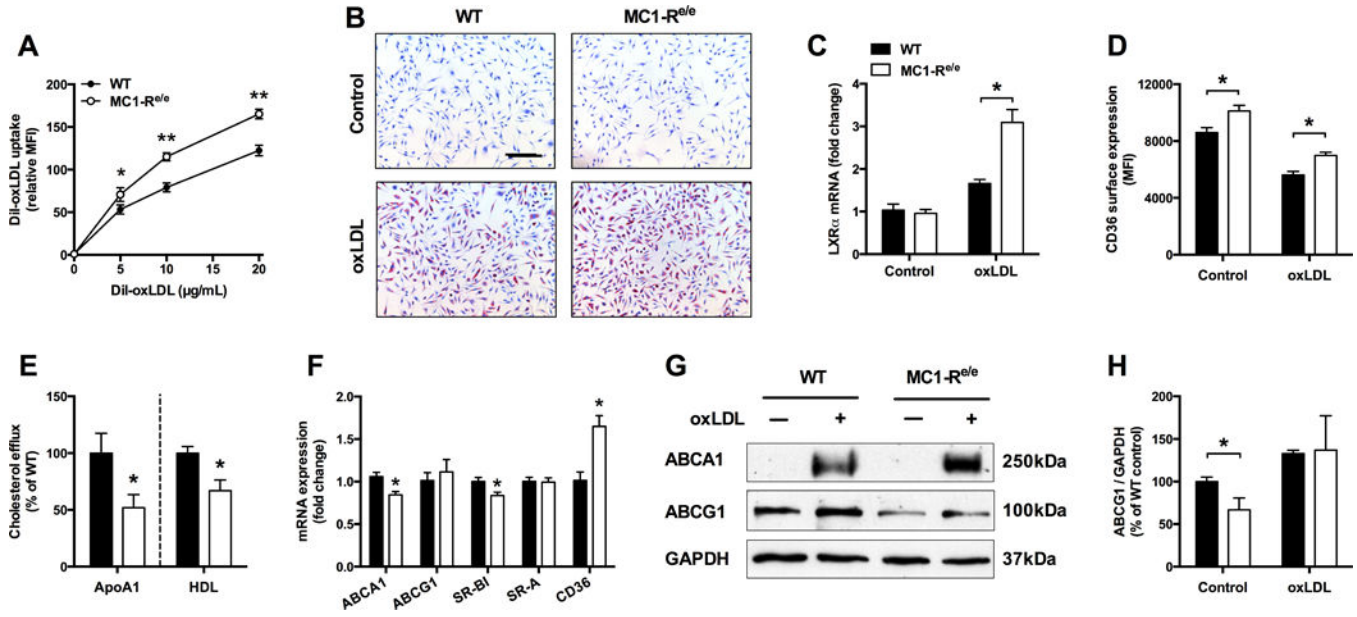

Figure 5. Dysfunctional MC1-R renders macrophages susceptible for increased cholesterol accumulation

A, Dil-oxLDL uptake in WT and MC1-R deficient BMDMs (MC1R$^{e/e}$) after 4h loading. **B**, Oil-Red-O staining of WT and MC1R$^{e/e}$ BMDMs under control conditions and in the oxLDL-loaded state (50μg/mL, 24h). Scale bar, 50μm. **C**, Quantitative RT-PCR analysis of LXRα expression in control and oxLDL-loaded (20μg/mL, 4h) macrophages. **D**, Quantification of CD36 surface expression by flow cytometry in WT and MC1R$^{e/e}$ BMDMs. **E**, Cholesterol efflux onto ApoA1 or HDL in WT and MC1R$^{e/e}$ BMDMs. Results are expressed as percentage of the efflux rate of WT cells. **F**, Quantitative RT-PCR analysis of ABCA1, ABCG1, SR-BI, SR-A and CD36 expression in WT and MC1R$^{e/e}$ BMDMs. **G** and **H**, Representative Western blots for ABCA1, ABCG1, and GAPDH (loading control) and quantification of ABCG protein levels in WT and MC1R$^{e/e}$ BMDMs under control conditions and after oxLDL loading (20μg/mL, 24h). * P<0.05 and ** P<0.01 versus WT. Data are mean ± SEM from 4 donor mice per genotype.

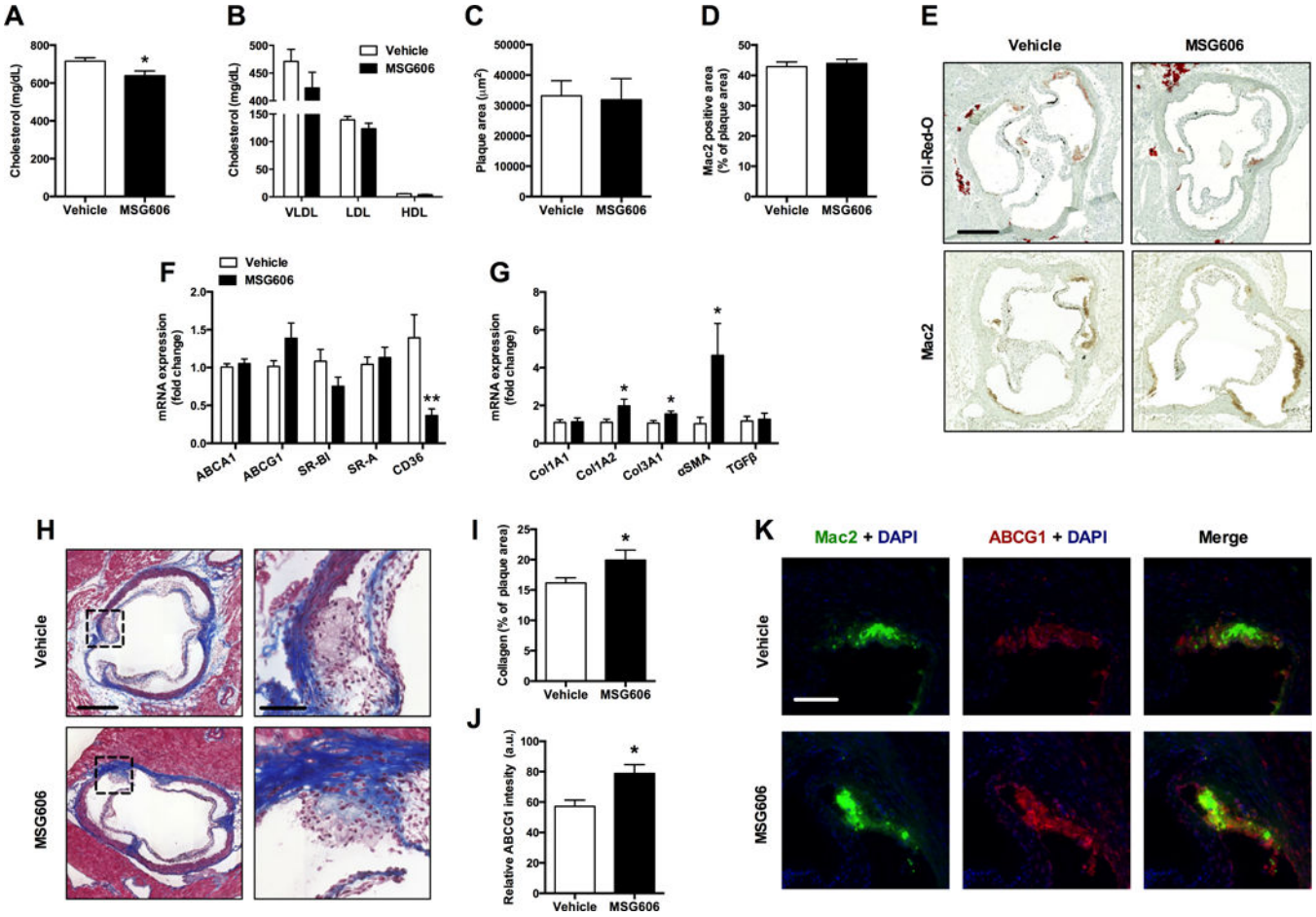

Figure 6. Chronic treatment with MSG606 does not affect plaque size but increases markers of plaque stability in atherosclerotic ApoE$^{-/-}$ mice

Plasma levels of total cholesterol (**A**) and VLDL, LDL and HDL cholesterol (**B**) in vehicle- and MSG606-treated mice. Quantification of total plaque area (**C**) and relative Mac-2 positive area (**D**). **E**, Representative Oil-Red-O and Mac-2-stained aortic root sections. Gene expression analysis of cholesterol transporters (**F**) and markers of plaque stability (**G**) in vehicle- and MSG606-treated mice. **H**, Representative Masson's trichrome stained sections from the aortic root. Scale bars, 500 μm (left panel) and 50 μm (right panel). **I**, Quantification of relative collagen content in atherosclerotic plaques. **J**, Quantification of relative ABCG1 fluorescence intensity in macrophage-rich plaque areas. **K**, Representative immunofluorescence images demonstrating staining for ABCG1 in Mac-2^{+} area of aortic root sections. * P<0.05 and ** P<0.01 versus Vehicle. Data are mean ± SEM. In **A**, n=18 (vehicle) and 14 (MSG606). In **B**, n=4 per group after pooling of 7 samples. In **C** through **J**, n=11 (vehicle) and 9 (MSG606).

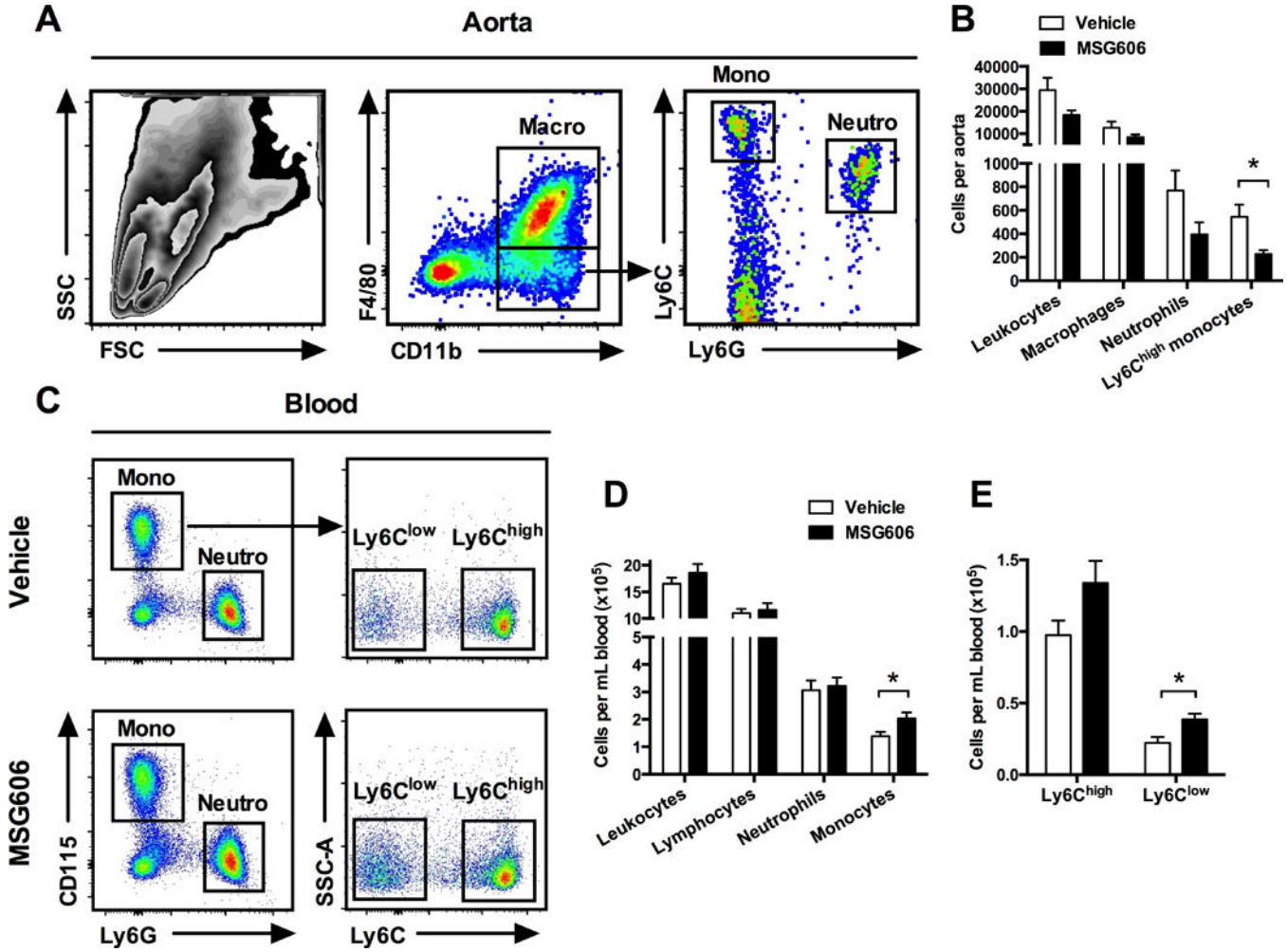

Figure 7. MSG606 treatment reduces monocyte counts in the aorta and modulates circulating monocyte profile

Representative flow cytometry results for the gating (**A**) and quantification (**B**) of total leukocytes ($CD45^+$), macrophages ($CD45^+$, $CD11b^+$, $F4/80^{high}$), neutrophils ($CD45^+$, $CD11b^+$, $Ly6G^+$) and $Ly6C^{high}$ monocytes ($CD45^+$, $CD11b^+$, $Ly6C^{high}$) in aortic lysates of vehicle- and MSG606-treated mice. **C** and **D**, Representative flow cytometry results and quantification of total leukocytes ($CD45^+$), lymphocytes ($CD45^+$, $CD11b^-$), neutrophils ($CD45^+$, $CD11b^+$, $Ly6G^+$) and monocytes ($CD45^+$, $CD11b^+$, $CD115^+$) in the blood. **E**, Quantification of $Ly6C^{high}$ and $Ly6C^{low}$ monocytes in the blood after gating for $CD115^+$ $Ly6G^-$ cells. * $P<0.05$ versus Vehicle. Data are mean ± SEM, n=11 (vehicle) and 9 (MSG606).